Distribution of lithostathine in the mouse lemur brain with aging and Alzheimer's-like pathology.

Stéphane Marchal, Laurent Givalois, Jean-Michel Verdier, Nadine Mestre-Francés

Title:

Distribution of lithostathine in the mouse lemur brain with aging and Alzheimer's-like pathology

Authors:

MARCHAL Stéphane, **GIVALOIS** Laurent, **VERDIER** Jean Michel and **MESTRE-FRANCES** Nadine.

Address:

University of Montpellier 2, Montpellier, F-34095 France; Inserm U710, Montpellier, F-34095 France; EPHE, Paris, F-75007 France.

Corresponding author:

Dr. Stéphane MARCHAL

Molecular Mechanisms in Neurodegenerative Dementia Laboratory,

U710 Inserm, EPHE, University of Montpellier 2

Place E. Bataillon,

34095 Montpellier, France.

Tel. (33) 467.14.38.15

Fax. (33) 467.14.33.86

E-mail: stephane.marchal@inserm.fr

ABSTRACT

We analyzed the cellular distribution of the pancreatic inflammatory protein lithostathine and its receptor EXTL3 in the brain of the lemurian primate *Microcebus murinus* which develops amyloid deposits along with aging. In adult animals (2-4.5 year-old), lithostathine and EXTL3 immunoreactivities were largely distributed in the whole brain, and more intensively in almost all cortical layers and hippocampal formation. Lithostathine was observed in the perikarya and neurites of cortical neurons but also in glial cells in the border of the ventricle and the corpus callosum. In healthy aged animals (8-13 year-old), highest densities of lithostathine containing cells were observed, mainly in occipital and parietal cortex. In aged animals with Aβ deposits, the increase in lithostathine immunoreactivity was lower as compared with aged animals. Noteworthly, lithostathine-immunopositive cells did almost never co-localize with Aβ plaques. In conclusion, lithostathine immunoreactivity in adult *Microcebus murinus* appeared ubiquitous and particularly in visual, sensorial and cognitive brain areas. Immunoreactivity increased with aging and appeared markedly affect in neuropathological conditions. Its possible neuroprotection or neurodegeneration role in Alzheimer pathology deserves therefore to be investigated.

Key words: lithostathine, lemur, β-amyloid deposit, EXTL3, Reg1

1. Introduction

Many degenerative diseases result from the aberrant polymerization and accumulation of specific proteins (Walker et al., 2006). These conformational diseases or proteopathies include neurological disorders such as Alzheimer's, Parkinson's, Huntington's and prion diseases, diverse systemic disorders, particularly amyloidoses including type II diabetes, light chain amyloidosis and cystic fibrosis (Aigelsreiter et al., 2007). At least 40 different proteins forming deposits have been described so far. Disorders involving protein deposition include a major protein component that forms the core, and additional species, including metal ions, glycosaminoglycans and glycoproteins. Many functions for these "pathological chaperones" have been reported, ranging from involvement in amyloidosis to a major role of stabilization of amyloid deposits. Their contribution to amyloid toxicity has been also investigated (Alexandrescu, 2005).

Among proteins that could contribute to amyloidosis, exocrine pancreatic protein named also lithostathine or Reg1 alpha, or pancreatic Thread Protein (PTP), is an inflammatory protein that forms deposits in pancreatic ducts of patients in chronic calcifying pancreatitis (De Caro et al., 1979). Originally identified as a secretory protein produced in pancreas by acinar cells (Iovanna et al., 1991), lithosthatine is very susceptible to self-proteolysis under specific pH conditions (Cerini et al., 1999). The cleavage produces a soluble N-terminal undecapeptide and a C-terminal part of 133 amino acids that precipitate and form protease-K-resistant fibrils at physiological pH (Gregoire et al., 2001). Although its physiological function in digestive organs remains debated (Bimmler et al., 1997; De Reggi et al., 1998), the protein tightly binds calcium carbonate crystals, suggesting an inhibitory activity on $CaCO_3$ crystal growth, thus preventing lithiasis (Bernard et al., 1992; Geider et al., 1996; Gerbaud et

al., 2000; Lee et al., 2003) . It has also been shown that acute pancreatitis induces Reg1 gene expression and protein production in the pancreas (Dusetti et al., 1996; Iovanna et al., 1991). This increase of Reg1 protein is associated with Reg1 receptor mRNA (Kobayashi et al., 2000) suggesting that an upregulation of the receptor expression may also be important in the proliferative response of pancreatic regeneration (Bluth et al., 2006). In gastric cells, the lithostathine protein was shown to be a regulator of gastric mucosal proliferation (Perfetti et al., 1994) and to function as a mitogenic and/or an antiapoptotic factor in the development of early gastric cancer (Sekikawa et al., 2005). Accordingly, Watanabe *et al*. (Watanabe et al., 1994) suggested that Reg1 protein has a trophic effect on isolated islet cells. More recently, a potential role of lithosthatine in normal and neoplastic germ cell proliferation has been also described (Mauro et al., 2008).

Interestingly, the presence of lithostathine was also evidenced in human brain (Ozturk et al., 1989; de la Monte et al., 1990). Protein expression depends on the developing human brain and the presence of neurofibrillary tangles in the pathogenesis of Alzheimer's disease (AD). More recently, accumulation of the protein was concomitant with the formation of Aβ and prion amyloid plaques in patients with AD and prion diseases (Duplan et al., 2001; Laurine et al., 2003). While the accumulation of the protein has been linked to the inflammatory process of the pathogenesis of AD (Duplan et al., 2001), little is known concerning the expression pattern of lithostathine in normal aging.

In the present investigation, we investigated the cellular distribution of lithostathine within the brain of a primate model of aging, *Microcebus murinus*. With age, loss of cholinergic neurones was evidenced in the basal telencephalon in some animals (Mestre and Bons, 1993). In addition, lemurian primate presents similar aging

characteristics as those observed in humans, such as modifications of the biological rhythms (Perret and Aujard, 2006), cognitive alterations (Picq, 1995; Picq, 2007; Bons et al., 2006) and cortical atrophy (Dhenain et al., 2000; Kraska et al., 2009) and it spontaneously develops numerous extracellular β-amyloid deposits in the cortical parenchyma (Bons et al., 1994; Mestre-Frances et al., 2000; Mestre-Frances et al., 1996). Rarely, neurofibrillary degeneration was observed in the cortical pyramidal neurons (Bons et al., 1991). In addition, accumulation of Tau proteins was also observed into the neocortex of young and old mouse lemurs (Mestre and Bons, 1993; Bons et al., 1995; Delacourte et al., 1995; Giannakopoulos et al., 1997) but not correlated to the presence of Aβ plaques (Giannakopoulos et al., 1997).

To determine the impact of aging and related pathology on lithostathine and its receptor brain expression, we performed a comparative analysis of lithostathine distribution in the brain of *Microcebus Murinus* as a function of age.

2. Material and methods

2.1. Brain tissue

The brains of 20 adult grey mouse lemurs *Microcebus murinus* aged from 1 to 13 years were collected. Three groups were considered: 8 adults (1-4.5 years-old), 6 healthy aged (5-13 years-old) (Perret, 1997) or 6 aged with amyloid plaques (5.5-13 years-old). Grey mouse lemurs were all born and kept in captivity within our breeding colony (Ecole Pratique des Hautes Etudes, license approval N^{br} 34-05-026-FS, France), according to the guidelines of the French Ethical Committee (Decree 87-848) and the European Community Directive (86/609/EEC). The animals were anesthetized with ketamine (150 mg/kg). Lemur brains were fixed by transcardially perfusion with 50 ml saline (0.9%) followed by 100 ml Antigenfix solution (Diapath,

France) or by immersion in Antigenfix solution for 24 hours. Brains were embedded in paraplast and sliced in 8 µm serial sagittal sections or cryoprotected (30% sucrose solution for 3 days), and quickly frozen into isopentane chilled in liquid nitrogen. Frozen brains were mounted on a cryostat (Leica, France) and serially cut into 10 µm sagittal sections.

2.2. Immunohistochemical procedures

2.2.1. Primary antibodies

The following antibodies were used to detect lithostathine immunopositive cells, its receptor or to identify various cell phenotypes in the brain: (1) rabbit polyclonal antibody against human lithosthatine protein (Litho-*romeo*, 1:100; (Duplan et al., 2001)); (2) goat IgG polyclonal antibody against lithostathine receptor (EXTL3, 1:100; R&D Systems, UK); (3) rabbit polyclonal antibody against amyloid peptide (1-42) (FCA3542, 1:1,000; Calbiochem, USA); (4) mouse IgG monoclonal antibody against glial fibrillary acidic protein (GFAP, 1:1,000; Sigma-Aldrich, France); (5) mouse IgG monoclonal antibody against human amyloid protein (1-42) (8G7, 1:100, Alexis Biochemicals, UK); (6) mouse IgG monoclonal antibody against β-tubulin protein (ßtub, 1:250; Sigma-Aldrich); (7) mouse IgG monoclonal antibody against microtubule associated protein (MAP2, 1:500; Sigma-Aldrich) and (8) mouse IgG monoclonal antibody against neuronal nuclei (NeuN, 1:250; Chemicon, USA).

2.2.2. Single immunoperoxidase labeling

Paraffin sections were dewaxed and hydrated through toluene and ethanol gradient and were then washed in water followed by immersion in hydrogen peroxide 3% for 30 min, rinsed in Tris-buffered saline (TBS), incubated with 3% goat serum containing 0.3% Triton X-100 in TBS for 30 min and then with anti-lithostathine

(1:100) or Aβ antibodies (8G7, FCA3542) (1:500) overnight at 4°C. After 3 washes in TBS, sections were incubated for 30 min in biotinylated goat or mouse anti-rabbit IgG (1:100, Vector USA). Subsequently, sections were washed again 3 times in TBS followed by 1h incubation in avidin-peroxydase complex (1:100, Vector). The sections were then washed in Tris buffer (0.5 M, pH 8.5) and reacted with diaminobenzidine tetrahydrocloride (DAB; 0.25 mg/ml, Sigma-Aldrich) in the same buffer containing 0.3% hydrogen peroxide. Standard immunohistochemical controls were performed including omission of the primary antibody, use of irrelevant secondary antibodies. No labeling was observed for controls.

2.2.3. Double immunoperoxidase labeling (DAB/histogreen)

The immunoperoxidase double labeling were carried out in the following two-step procedure. First, DAB was used for the detection of lithostathine as described above. The second step consisted of incubation of sections with formic acid (80%) for 10 min. After 5 washes in water, sections were then incubated with 3% goat serum containing 0.3% Triton X-100 in TBS for 30 min and then with $A\beta_{1-42}$ antibody (FCA3542, 1:500) overnight at 4°C. After successive steps of washing, incubation with biotinylated anti-rabbit IgG (1:100) and with avidin-peroxidase complex, respectively, the HistoGreen substrate kit (HISTOPRIME, AbCys, France) was used for detection of $A\beta_{1-42}$-immunoreactive deposits.

2.2.4. Double immunofluorescent labeling

For double immunofluorescent labeling, sections were incubated in a cocktail of monoclonal and polyclonal primary antibodies followed by secondary antibodies linked to different fluorophores. The lithostathine antibody (1:100) was co-incubated with either anti-NeuN (1:250), anti-MAP2 (1:500), anti-βtub (1:250) or anti-GFAP

(1:500). The sections were prepared by using the same procedure as the single-labeled sections. The sections were incubated in primary antibodies overnight at 4°C, washed and then incubated in species-specific fluorescent secondary antibody directly linked to anti-rabbit and anti-goat AlexaFluor 488 (1:2,000, Molecular Probes, Leiden, The Netherlands), anti-rabbit AlexaFluor 555 (1:2,000) or anti-mouse Cy3 (1:2,000, Jackson ImmunoResearch Inc., USA). The nuclei were counterstained with 4',6'-diamino-2-phenylindole (DAPI, Molecular Probes). To detect any cross-reactivity in the double labeling experiments, each primary antibody in the pair was incubated with both secondary antibodies to be used in the double labeling.

2.3. Analysis

The main aim of the experiments carried out in this study was to determine the regional and cellular distribution of lithostathine in the grey mouse lemur brain.

First single immunoperoxidase labeled sections were examined by light microscopy and qualitative observations were recorded. The quantitative study in cortical areas was performed using standardized image analysis and mapping system from Explora Nova™ (Mercator software). Paraffin-embedded sections from medial to temporal hemisphere were investigated every 400µm for cell counting from the coordinates L:0.6mm to L:3.40mm of the mouse lemur brains (Bons et al., 1998). Each cortical lithostathine immunoreactive cell showing labelled perikaria and neurites (fig. 1 C-G) was plotted on each section (ie, 8 sections per animal). From experimental data, software facilities generates a map for each section (cf fig.5 A, B, I, J). The count of the immunoreactive cells was done by two different scientists unaware experimental conditions and independently each other.

Double-labeling immunoperoxidase experiments using sections labeled with antibodies against lithostathine and $A\beta_{1-42}$ were carried out to investigate the

colocalization of proteins. Double-immunofluorescent staining for lithostathine and EXTL3, NeuN, MAP2, βtub, and GFAP were observed with a Leica fluorescent microscope (DMR; Leica).

2.4. Statistical analysis

The number of positive cells/section was presented as mean ± SEM. Comparisons were performed by a one-way ANOVA (Statview 4.5) followed by a Fisher's PLSD test. $p< 0.05$ was considered significant.

3. RESULTS

3.1. Regional distribution of lithostathine immunoreactivity

The distribution of lithostathine immunoreactivity was assessed by examining different levels of lemur brain tissue from medial (Fig.1A) to temporal (Fig.1B) sections. Fibers within the white matter were immunopositive: corpus callosum, fornix, internal capsule, anterior part of the anterior commissure, olfactory tract, optic chiasma, posterior commissure, pedunculus cerebri, tractus tegmenti centralis, pons, tractus solitarius, pedunculus cerebellaris. Positive cells were observed in the olfactory tubercle, into piriform cortex, entorhinal cortex and amygdale (Fig.1A-B).

Within the grey matter, immunopositive cells were scattered into cerebral neocortex, in layers III (external pyramidal layer) and V (internal pyramidal layer). Strongly positive cells were also observed in layer II (external granular layer) and IV (internal granular layer) (Fig.1C, E, F).

In subcortical areas, some cells were stained in the anterior hypothalamic area and into the reticular nucleus of the thalamus (Fig.1D). The most abundant population of lithostathine-positive cells was evidenced in superior and inferior colliculi where magnocellular pyramidal cells were strongly immunoreactive (Fig.1G). Magnocellular cells were also detected in brainstem into the locus coeruleus

Morphologically, lithostathine-positive cells were mainly large pyramidal cells in layer III and V (Fig.2A, C, E-G) and small-size cells in other layers (Fig.2A, C). None of the immunopositive cells showed lithostathine staining in their nuclei. Positive cells were numerous in parietal cortex and more abundant in frontal, occipital and temporal cortex. In the hippocampus, we essentially observed cells in the ventral part, in CA2 area (Fig.2B, H). Fibers were detected in the subiculum entering into the ventral part of the hippocampus and numerous synaptic labeling were observed in CA2 and CA3 layers (Fig.2D). In the dorsal part, no immunofluorescent cells were detected. Control sections in which the primary antibody was omitted showed no immunoreactivity. The control experiments showed that the secondary antibodies did not cross-react with each other (data not shown).

In old mouse lemurs, lithostathine was generally observed in the same areas with discrepancies in location in cortical areas compared to adults. In old animals, protein accumulation was essentially observed in the parietal and occipital cortex whereas in adult brains, protein accumulation was rather observed in all cortical areas. Old mouse lemur brains were also characterized by strong accumulation of lipofuscin granules into the neurons of cortex and subcortical structures (data not shown).

3.2. Cellular localization and morphology

Neuronal and glial markers were used to determine the phenotype of cells that displayed lithostathine immunoreactivity in the grey mouse lemur brain (Fig.2). Lithostathine labeling was mainly observed in the cytoplasm of neurons and also into almost all of neurites (see also Fig.1), evidenced by MAP2 (Fig.2A-B) and β-tubulin (Fig.2G-H) antibodies. For old animals, the location of lithostathine was rather detected at the vicinity of the membrane and not more in the cytoplasm (fig 5.H). The

neuronal marker NeuN (Fig.2C-F) stained almost all the immunopositive cells of the brain and GFAP antibody (Fig.2I-L) evidenced few lithostathine-positive ependymal cells of the lateral ventricle (Fig.2J) and some astrocytes into the fornix (Fig.2K) and optic chiasma (Fig.2L).

3.3. Regional localization of lithostathine receptor EXTL3

Pyramidal neurons and interneurons of the cerebral cortex were immunostained by EXTL3 antibody. Immunoreactivity was more abundant in temporo-occipital, fronto-temporal and medial occipital area than in medial parietal area (Fig.3A-B, D, G, H). Olfactory areas as olfactory bulb, olfactory anterior nucleus, olfactory tubercle, pyriform cortex and entorhinal cortex showed numerous immunoreactive neurons. The dorsal part (Fig.3C) and the ventral part (Fig.3F) of the hippocampus showed some neurons labeled by EXTL3 antibody. Intense labeling was detected in the medial thalamus (dorsomedian, anteroventral nuclei) and also in lateral thalamic nuclei, geniculate and reticularis nuclei (Fig.3F). The anterior hypothalamic area and preoptic nucleus showed numerous immunostained neurons. In the mesencephalic areas, important labeling was detected in inferior and superior colliculi (Fig.3E). Lithostathine receptors were observed in the neurons of the red nucleus and substantia nigra nuclei and were scattered into the brainstem but essentially in the central interpeduncularis nucleus, the lateral lemniscus, the reticular tegmenti pontis nucleus, the raphe nuclei and in the vestibular nuclei. Using double immunofluorescence labeling, immunocytohistochemistry indicated that lithostathine and its receptor are localized in the same pyramidal neurons of hippocampic CA areas and cortex (Fig 3H). Specifically, the punctiform labeling suggested that lithostathine-EXTL3 interaction were localized predominantly to the endoplasmic

reticulum or Golgi, as already described for EXTL3 protein immunolabeling in cellular models or in *Drosophila* (Han et al., 2004; McCormick et al., 2000; Mizuno et al., 2001).

3.4. Comparative distribution of cortical lithostathine neurons in adult, aged and aged animals with amyloid plaques

The presence of lithostathine was investigated in correlation with amyloid deposition by double labeling immunohistochemistry. In comparison to adult and healthy old lemurs (Fig. 4A,B), some old animals presented diffuse amyloid deposits (Fig. 4C) or compact plaques (Fig. 4D). In some animals, we observed lithostathine-positive neurons in close contact with amyloid deposits (Fig. 4E-H) but in most cases, lithostathine immunoreactivity was detected in areas with few amyloid plaques (Fig. 4I-K).

As shown in figure 5, the number of cells with lithostathine staining was statistically significant between the different groups analyzed ($F_{2,17}$ = 24.4; $p < 0.001$). Notably, the number of positive cells per section was significantly increased by 10 fold in old lemurs ($p < 0.01$ *vs.* adult animals) and by 4.5 fold in old animals with amyloid plaques ($p < 0.01$ *vs* adult animals). Nevertheless, a decrease by 2.4-fold was observed when compared with healthy old lemurs ($p < 0.01$; Fig. 5).

4. DISCUSSION

Few investigations reported the presence of lithostathine in the normal brain. Studies were mostly dedicated to Alzheimer's disease (de la Monte et al., 1990; Duplan et al., 2001; Ozturk et al., 1989) or Creutzfeldt-Jakob disease (CJD) (Laurine et al., 2003), but not to normal aging.

In the present investigation, we examined the presence of lithostathine and its receptor in the brain of the grey mouse lemur *Microcebus murinus*. Among the twelve old animals tested, six of them showed amyloid plaques but no neurofibrillary tangles nor cortical atrophy (data not shown). Unfortunately, cognitive performances were not investigated in those animals.

Lithostathine immunoreactivity was observed in perikarya and neurites of cortical pyramidal neurons, but also in some glial cells particularly in the corpus callosum, as previously described in human brain (Ozturk et al., 1989). In the normal adult brain, a low level of protein immunoreactivity was detected. However, with aging, a strong accumulation of protein occurred in old mouse lemurs with or without amyloid plaques. In human, high levels of lithostathine-containing neurons was observed only for AD brains (de la Monte et al., 1990; Ozturk et al., 1989). These authors suggested that accumulation of lithostathine precedes or occurs independently of neurofibrillary tangles. They concluded that lithostathine was related to the evolution of AD lesions because immunolabeling was observed in AD patients or patients with Down Syndrome (DS), but not in normal brain. In addition, they observed that the density of the lithostathine-containing neurons was proportional to the distributions of neurofibrillary tangles in AD and DS.

Lithostathine-immunoreactive neurons were observed at the vicinity of diffuse plaques but never detected into amyloid plaques or neurofibrillary tangles as it has been shown earlier (de la Monte et al., 1990; Duplan et al., 2001; Ozturk et al., 1989). By contrast, our data rather suggest that accumulation of lithostathine in old animals is not AD-specific but occurs mainly during normal aging, showing an unexpected increase compared to AD-like animals. The observation of high levels of lithostathine immunoreactivity in cortical areas of healthy aged animals deserves discussion. One

question to be addressed is why lithostathine accumulates in normal brain during aging ? First, it could be considered that the deficit of lithostathine level observed in AD-like aged animals in comparison to healthy elderly mouse lemurs and the location of amyloid plaques observed in areas devoid of lithostathine-reactive neurons suggest a protective role of lithostathine, as previously reported in peripheral tissues (Orelle et al., 1992; Sekikawa et al., 2005; Viterbo et al., 2009). This function may be related to a putative involvement of lithostathine in plasticity mechanisms as suggested by De La Monte *et al*. (de la Monte et al., 1990) or evidenced for an homologous regenerating protein Reg2 in central nervous system (Nishimune et al., 2000). In contrast, based on the pro-inflammatory property of lithostathine and its link to pro-inflammatory cytokines overexpression (Duplan et al., 2001), we propose that accumulation of lithostathine in the brain would also be an indirect consequence of peculiar chronic inflammatory status during aging (Franceschi and Bonafe, 2003; Giunta et al., 2008; Giunta, 2006). All in all, these findings indicate that lithostathine represents an interesting protein to be investigated for its role in aging.

Acknowledgements

We are especially grateful to Dr Tangui Maurice for helpful comments, Dr Susanna Malmström for improving english.

Disclosure statements

In relation to the present study, the authors declare that, except for income received from their primary employer, no financial support or compensation has been received from any individual or corporate entity over the past three years for research or

professional service and there are no personal financial holdings that could be perceived as constituting a potential conflict of interest. In addition, funding for this study was provided by recurrent funds from the INSERM (France). INSERM had no further role in study design; in the collection, analysis and interpretation of data; in the writing of the report; and in the decision to submit the paper for publication.

The authors state that there are no actual or potential conflicts of interest.

References

Aigelsreiter, A., Janig, E., Stumptner, C., Fuchsbichler, A., Zatloukal, K. and Denk, H. (2007). How a cell deals with abnormal proteins. Pathogenetic mechanisms in protein aggregation diseases. Pathobiology 74, 145-58.

Alexandrescu, A. T. (2005). Amyloid accomplices and enforcers. Protein Sci 14, 1-12.

Bernard, J. P., Adrich, Z., Montalto, G., De Caro, A., De Reggi, M., Sarles, H. and Dagorn, J. C. (1992). Inhibition of nucleation and crystal growth of calcium carbonate by human lithostathine. Gastroenterology 103, 1277-84.

Bimmler, D., Graf, R., Scheele, G. A. and Frick, T. W. (1997). Pancreatic stone protein (lithostathine), a physiologically relevant pancreatic calcium carbonate crystal inhibitor? J Biol Chem 272, 3073-82.

Bluth, M. H., Patel, S. A., Dieckgraefe, B. K., Okamoto, H. and Zenilman, M. E. (2006). Pancreatic regenerating protein (reg I) and reg I receptor mRNA are upregulated in rat pancreas after induction of acute pancreatitis. World J Gastroenterol 12, 4511-6.

Bons, N., Jallageas, V., Silhol, S., Mestre-Frances, N., Petter, A. and Delacourte, A. (1995). Immunocytochemical characterization of Tau proteins during cerebral aging of the lemurian primate Microcebus murinus. C R Acad Sci III 318, 741-7.

Bons, N., Mestre, N. and Petter, A. (1991). Presence of neuritic plaques and neurofibrillary changes in the cerebral cortex of an aged lemuride primate. C R Acad Sci III 313, 213-9.

Bons, N., Mestre, N., Ritchie, K., Petter, A., Podlisny, M. and Selkoe, D. (1994). Identification of amyloid beta protein in the brain of the small, short-lived lemurian primate Microcebus murinus. Neurobiol Aging 15, 215-20.

Bons, N., Rieger, F., Prudhomme, D., Fisher, A. and Krause, K. H. (2006). Microcebus murinus: a useful primate model for human cerebral aging and Alzheimer's disease? Genes Brain Behav 5, 120-30.

Bons, N., Silhol, S., Barbie, V., Mestre-Frances, N. and Albe-Fessard, D. (1998). A stereotaxic atlas of the grey lesser mouse lemur brain (Microcebus murinus). Brain Res Bull 46, 1-173.

Cerini, C., Peyrot, V., Garnier, C., Duplan, L., Veesler, S., Le Caer, J. P., Bernard, J. P., Bouteille, H., Michel, R., Vazi, A., Dupuy, P., Michel, B., Berland, Y. and Verdier, J. M. (1999). Biophysical characterization of lithostathine. Evidences for a polymeric structure at physiological pH and a proteolysis mechanism leading to the formation of fibrils. J Biol Chem 274, 22266-74.

De Caro, A., Lohse, J. and Sarles, H. (1979). Characterization of a protein isolated from pancreatic calculi of men suffering from chronic calcifying pancreatitis. Biochem Biophys Res Commun 87, 1176-82.

de la Monte, S. M., Ozturk, M. and Wands, J. R. (1990). Enhanced expression of an exocrine pancreatic protein in Alzheimer's disease and the developing human brain. J Clin Invest 86, 1004-13.

De Reggi, M., Gharib, B., Patard, L. and Stoven, V. (1998). Lithostathine, the presumed pancreatic stone inhibitor, does not interact specifically with calcium carbonate crystals. J Biol Chem 273, 4967-71.

Delacourte, A., Sautiere, P. E., Wattez, A., Mourton-Gilles, C., Petter, A. and Bons, N. (1995). Biochemical characterization of Tau proteins during cerebral aging of the lemurian primate Microcebus murinus. C R Acad Sci III 318, 85-9.

Dhenain, M., Michot, J. L., Privat, N., Picq, J. L., Boller, F., Duyckaerts, C. and Volk, A. (2000). MRI description of cerebral atrophy in mouse lemur primates. Neurobiol Aging 21, 81-8.

Duplan, L., Michel, B., Boucraut, J., Barthellemy, S., Desplat-Jego, S., Marin, V., Gambarelli, D., Bernard, D., Berthezene, P., Alescio-Lautier, B. and Verdier, J. M. (2001). Lithostathine and pancreatitis-associated protein are involved in the very early stages of Alzheimer's disease. Neurobiol Aging 22, 79-88.

Dusetti, N. J., Mallo, G. V., Ortiz, E. M., Keim, V., Dagorn, J. C. and Iovanna, J. L. (1996). Induction of lithostathine/reg mRNA expression by serum from rats with acute pancreatitis and cytokines in pancreatic acinar AR-42J cells. Arch Biochem Biophys 330, 129-32.

Franceschi, C. and Bonafe, M. (2003). Centenarians as a model for healthy aging. Biochem Soc Trans 31, 457-61.

Geider, S., Dussol, B., Nitsche, S., Veesler, S., Berthezene, P., Dupuy, P., Astier, J. P., Boistelle, R., Berland, Y., Dagorn, J. C. and Verdier, J. M. (1996). Calcium carbonate crystals promote calcium oxalate crystallization by heterogeneous or epitaxial nucleation: possible involvement in the control of urinary lithogenesis. Calcif Tissue Int 59, 33-7.

Gerbaud, V., Pignol, D., Loret, E., Bertrand, J. A., Berland, Y., Fontecilla-Camps, J. C., Canselier, J. P., Gabas, N. and Verdier, J. M. (2000). Mechanism of calcite crystal growth inhibition by the N-terminal undecapeptide of lithostathine. J Biol Chem 275, 1057-64.

Giannakopoulos, P., Silhol, S., Jallageas, V., Mallet, J., Bons, N., Bouras, C. and Delaere, P. (1997). Quantitative analysis of tau protein-immunoreactive accumulations and beta amyloid protein deposits in the cerebral cortex of the mouse lemur, Microcebus murinus. Acta Neuropathol 94, 131-9.

Giunta, B., Fernandez, F., Nikolic, W. V., Obregon, D., Rrapo, E., Town, T. and Tan, J. (2008). Inflammaging as a prodrome to Alzheimer's disease. J Neuroinflammation 5, 51.

Giunta, S. (2006). Is inflammaging an auto[innate]immunity subclinical syndrome? Immun Ageing 3, 12.

Gregoire, C., Marco, S., Thimonier, J., Duplan, L., Laurine, E., Chauvin, J. P., Michel, B., Peyrot, V. and Verdier, J. M. (2001). Three-dimensional structure of the lithostathine protofibril, a protein involved in Alzheimer's disease. Embo J 20, 3313-21.

Han, C., Belenkaya, T. Y., Khodoun, M., Tauchi, M., Lin, X. and Lin, X. (2004). Distinct and collaborative roles of Drosophila EXT family proteins in morphogen signalling and gradient formation. Development 131, 1563-75.

Iovanna, J. L., Keim, V., Michel, R. and Dagorn, J. C. (1991). Pancreatic gene expression is altered during acute experimental pancreatitis in the rat. Am J Physiol 261, G485-9.

Kobayashi, S., Akiyama, T., Nata, K., Abe, M., Tajima, M., Shervani, N. J., Unno, M., Matsuno, S., Sasaki, H., Takasawa, S. and Okamoto, H. (2000). Identification of a receptor for reg (regenerating gene) protein, a pancreatic beta-cell regeneration factor. J Biol Chem 275, 10723-6.

Kraska, A., Dorieux, O., Picq, J. L., Petit, F., Bourrin, E., Chenu, E., Volk, A., Perret, M., Hantraye, P., Mestre-Frances, N., Aujard, F. and Dhenain, M. (2009). Age-associated cerebral atrophy in mouse lemur primates. Neurobiol Aging.

Laurine, E., Gregoire, C., Fandrich, M., Engemann, S., Marchal, S., Thion, L., Mohr, M., Monsarrat, B., Michel, B., Dobson, C. M., Wanker, E., Erard, M. and Verdier, J. M. (2003). Lithostathine quadruple-helical filaments form proteinase K-resistant deposits in Creutzfeldt-Jakob disease. J Biol Chem 278, 51770-8.

Lee, B. I., Mustafi, D., Cho, W. and Nakagawa, Y. (2003). Characterization of calcium binding properties of lithostathine. J Biol Inorg Chem 8, 341-7.

Mauro, V., Carette, D., Chevallier, D., Michiels, J. F., Segretain, D., Pointis, G. and Senegas-Balas, F. (2008). Reg I protein in healthy and seminoma human testis. Histol Histopathol 23, 1195-203.

McCormick, C., Duncan, G., Goutsos, K. T. and Tufaro, F. (2000). The putative tumor suppressors EXT1 and EXT2 form a stable complex that accumulates in the Golgi apparatus and catalyzes the synthesis of heparan sulfate. Proc Natl Acad Sci U S A 97, 668-73.

Mestre-Frances, N., Keller, E., Calenda, A., Barelli, H., Checler, F. and Bons, N. (2000). Immunohistochemical analysis of cerebral cortical and vascular lesions in the primate Microcebus murinus reveal distinct amyloid beta1-42 and beta1-40 immunoreactivity profiles. Neurobiol Dis 7, 1-8.

Mestre-Frances, N., Silhol, S. and Bons, N. (1996). Evolution of beta-amyloid deposits in the cerebral cortex of Microcebus murinus lemurian primate. Alzheimer's Res. 2, 19-28.

Mestre, N. and Bons, N. (1993). Age-related cytological changes and neuronal loss in basal forebrain cholinergic neurons in Microcebus marinus (Lemurian, primate). Neurodegeneration 2, 25-32.

Mizuno, K., Irie, S. and Sato, T. A. (2001). Overexpression of EXTL3/EXTR1 enhances NF-kappaB activity induced by TNF-alpha. Cell Signal 13, 125-30.

Nishimune, H., Vasseur, S., Wiese, S., Birling, M. C., Holtmann, B., Sendtner, M., Iovanna, J. L. and Henderson, C. E. (2000). Reg-2 is a motoneuron neurotrophic factor and a signalling intermediate in the CNTF survival pathway. Nat Cell Biol 2, 906-14.

Orelle, B., Keim, V., Masciotra, L., Dagorn, J. C. and Iovanna, J. L. (1992). Human pancreatitis-associated protein. Messenger RNA cloning and expression in pancreatic diseases. J Clin Invest 90, 2284-91.

Ozturk, M., de la Monte, S. M., Gross, J. and Wands, J. R. (1989). Elevated levels of an exocrine pancreatic secretory protein in Alzheimer disease brain. Proc Natl Acad Sci U S A 86, 419-23.

Perfetti, R., Egan, J. M., Zenilman, M. E. and Shuldiner, A. R. (1994). Expression of the regenerating gene in the pancreas of aging mice. Transplant Proc 26, 733.

Perret, M. (1997). Change in photoperiodic cycle affects life span in a prosimian primate (Microcebus murinus). J Biol Rhythms 12, 136-45.

Perret, M. and Aujard, F. (2006). [Aging and biological rhythms in primates]. Med Sci (Paris) 22, 279-83.

Picq, J. L. (1995). Effects of aging upon recent memory in Microcebus murinus. Aging (Milano) 7, 17-22.

Picq, J. L. (2007). Aging affects executive functions and memory in mouse lemur primates. Exp Gerontol 42, 223-32.

Sekikawa, A., Fukui, H., Fujii, S., Takeda, J., Nanakin, A., Hisatsune, H., Seno, H., Takasawa, S., Okamoto, H., Fujimori, T. and Chiba, T. (2005). REG Ialpha protein may function as a trophic and/or anti-apoptotic factor in the development of gastric cancer. Gastroenterology 128, 642-53.

Viterbo, D., Callender, G. E., DiMaio, T., Mueller, C. M., Smith-Norowitz, T., Zenilman, M. E. and Bluth, M. H. (2009). Administration of anti-Reg I and anti-PAPII antibodies worsens pancreatitis. Jop 10, 15-23.

Walker, L. C., Levine, H., 3rd, Mattson, M. P. and Jucker, M. (2006). Inducible proteopathies. Trends Neurosci 29, 438-43.

Watanabe, T., Yonemura, Y., Yonekura, H., Suzuki, Y., Miyashita, H., Sugiyama, K., Moriizumi, S., Unno, M., Tanaka, O., Kondo, H. and et al. (1994). Pancreatic beta-cell replication and amelioration of surgical diabetes by Reg protein. Proc Natl Acad Sci U S A 91, 3589-92.

Figure legends

Figure 1:

Lithostathine distribution in the *Microcebus murinus* brain

Distribution of lithostathine immunopositive neurons from medial (A) to temporal (B) sections of mouse lemur brain atlas: neurons are largely distributed in the colliculi (c), cortex (cx), the hypothalamic area (h) and locus coeruleus (lc). Temporal section showed that lithostathine immunoreactive neurons were also present in thalamus (t), olfactory structures (olf) and hippocampus (hp). Immunostaining of lithostathine neurons in layers II (C) and in perikarya and neuritis of pyramidal cells in layer IV and V (E,F), in thalamus (D) and in colliculus (G). Scale bar: 50 µm.

Figure 2:

Cellular localization of lithostathine.

Double immunostaining experiments were used to investigate the cellular localization of lithostathine. Specific antibody against lithostathine was revealed with Alexa Fluor 488-labeled secondary antibodies (green immunolabeling) and specific antibodies against MAP2, β-tubulin (βtub), NeuN or GFAP were detected with Cy3-labeled secondary antibodies. The nuclei were counterstained with 4',6'-diamino-2-phenylindole (DAPI). Lithostathine was observed in perikarya and neurites of neurons, in neocortical areas (A,C,E-G), in hippocampus (B,D,H) in astrocytes into the fornix (K) and optic chiasma (L) and in ependymar cells of the lateral ventricle (J). Scale bar: 30 µm.

Figure 3:

Regional and cellular distribution of the lithostathine receptor EXTL3 in the *Microcebus murinus* brain.

Representative overview of EXTL3 distribution from medial (A) to temporal (B) sections: EXTL3 positive cells are largely distributed into the cortical areas (cx) but also in subcortical areas: olfactory structures (olf), thalamic (t) and hypothalamic nuclei (h), ventral tegmental area (vta), colliculi (c) and brainstem (b). Immunoreactive cells were detected in pyramidal neurons of hippocampic CA areas (C,F), in pyramidal neurons of the cortex (D,G,H), and in thalamus (E). EXTL3 (green) was observed in the neurons that showed lithosthatine immunoreactivity (red) (H1-3).

Figure 4:

Lithosthatine immunostaining in cortical areas of adult, healthy old and old lemur with amyloid plaques.

Figure represents the cortical distribution of lithostathine immunostaining in adult (A), healthy old (B) and old lemur with amyloid plaques (J). The presence of amyloid plaques was detected by 8G7 (C, G) or FCA3542 (D) antibodies. Lithostathine neurons, visualized using 3,3' diaminobenzidine as the chromogen (brown) were sometimes detected in the vicinity of amyloid deposits (histogreen) (E,F,H). Distribution of neurons exhibiting lithostathine (I) and localization of Aβ deposits in cerebral neocortex (J) and merge (K) of old-Aβ lemur brain. Mapping of neurons and Aβ plaques were performed using Mercator software (Explora Nova, La Rochelle, France)

Figure 5:

Quantitative comparison of immunostained neurons for lithostathine in adult, healthy old and old-Aβ lemur brains.

Paraffin-embedded sections of adult brain were immunostained with the polyclonal rabbit antibody against human lithostathine and neurons of cortical brain area were counted using Mercator software. The values are mean ± SEM. Ns. no significant and ∗∗ $p<0.01$ *vs* adult animals, and ++ $p<0.01$ *vs* healthy old animals. Adult animals: ID199 (1.5 year-old), ID484 (2 year-old), ID489 (2 year-old), ID155 (2.5 year-old), ID156 (2.5 year-old), ID202 (3 year-old), ID479 (3 year-old) and ID551 (4 year-old); healthy old lemurs: ID475 (8 year-old), ID486 (9 year-old), ID528 (9 year-old), ID921 (9 year-old), ID435 (10 year-old), ID468 (13 year-old); old Aβ lemurs: ID463 (5.5 year-old), ID988 (8 year-old), ID973 (9 year-old), ID473 (10 year-old), ID516 (10 year-old), ID896 (13 year-old)

Fig.1

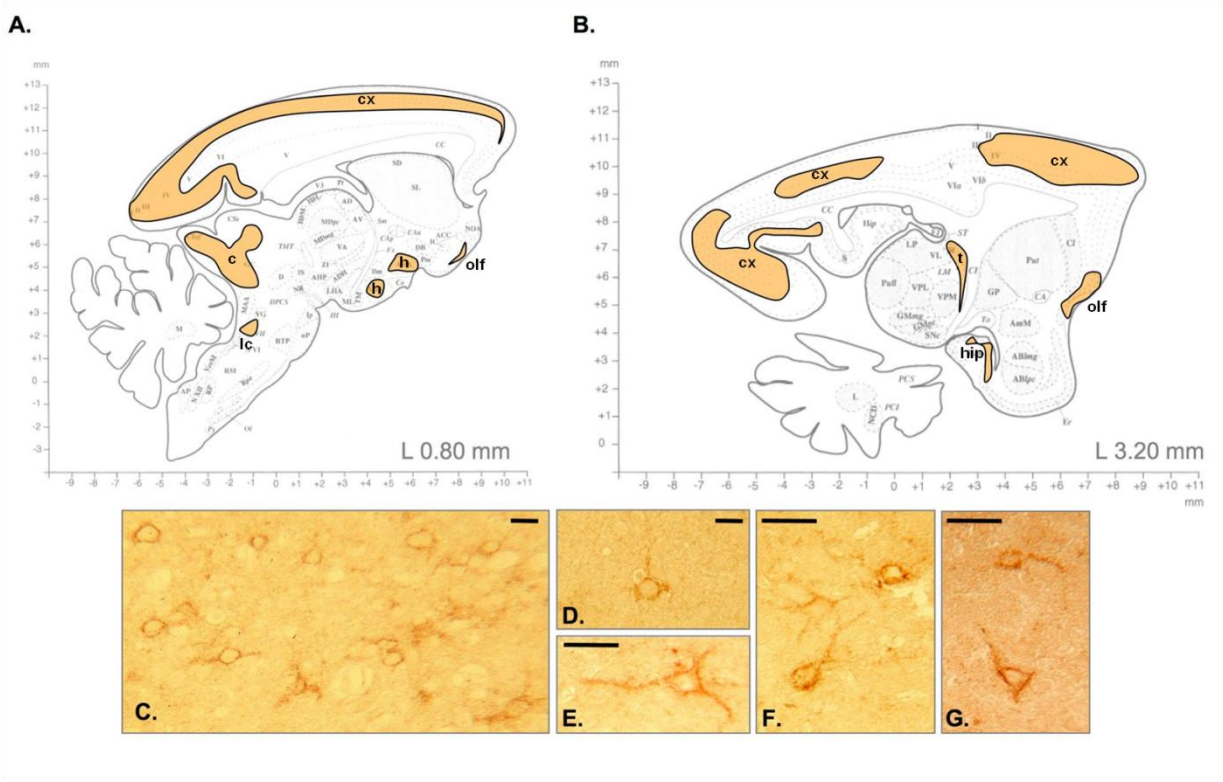

Fig.2A

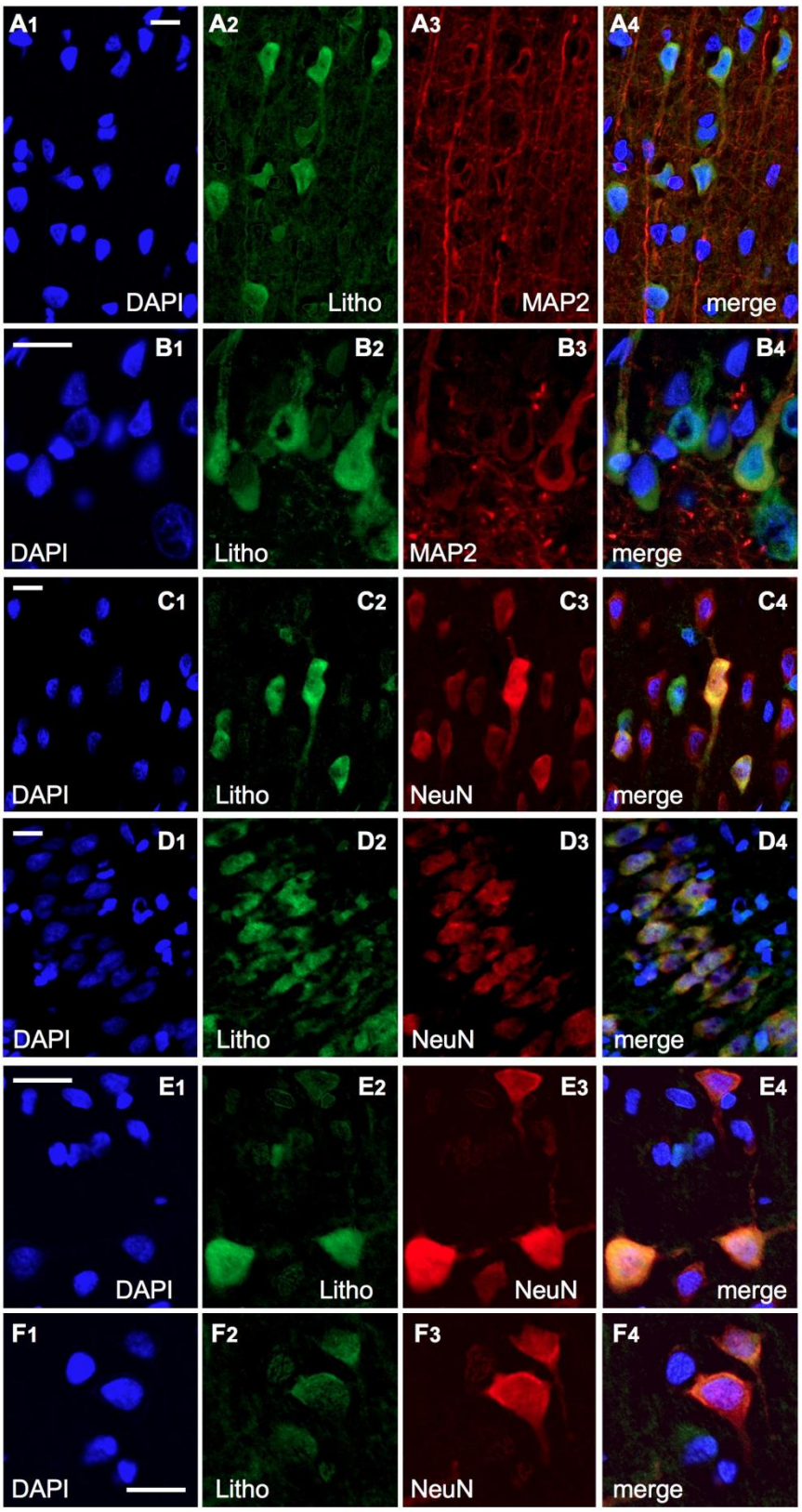
A1
DAPI
A2
Litho
A3
MAP2
A4
merge
B1
DAPI
B2
Litho
B3
MAP2
B4
merge
C1
DAPI
C2
Litho
C3
NeuN
C4
merge
D1
DAPI
D2
Litho
D3
NeuN
D4
merge
E1
DAPI
E2
Litho
E3
NeuN
E4
merge
F1
DAPI
F2
Litho
F3
NeuN
F4
merge

Fig2.B

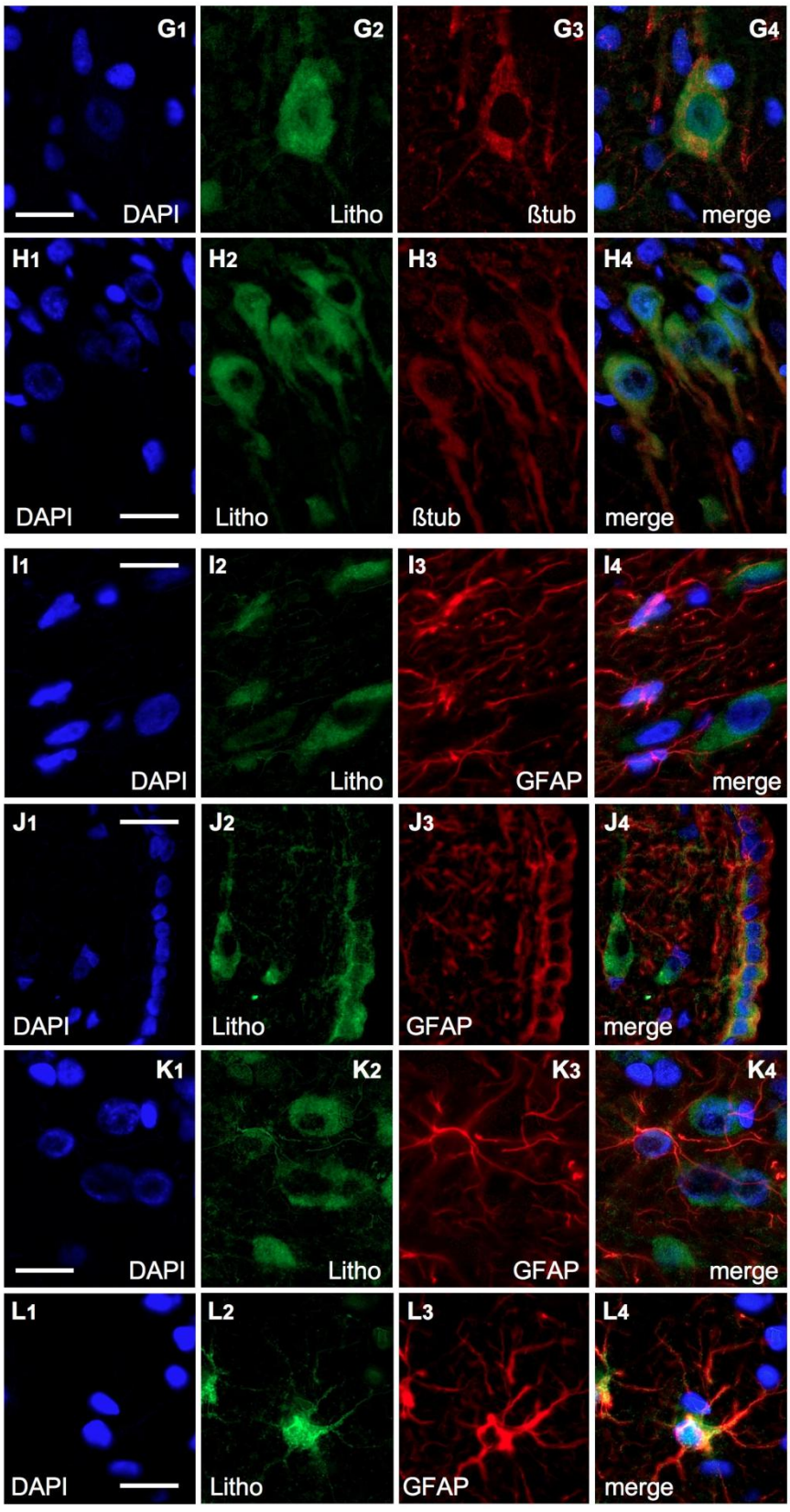
G1
DAPI
G2
Litho
G3
ßtub
G4
merge
H1
DAPI
H2
Litho
H3
ßtub
H4
merge
I1
DAPI
I2
Litho
I3
GFAP
I4
merge
J1
DAPI
J2
Litho
J3
GFAP
J4
merge
K1
DAPI
K2
Litho
K3
GFAP
K4
merge
L1
DAPI
L2
Litho
L3
GFAP
L4
merge

Fig.3

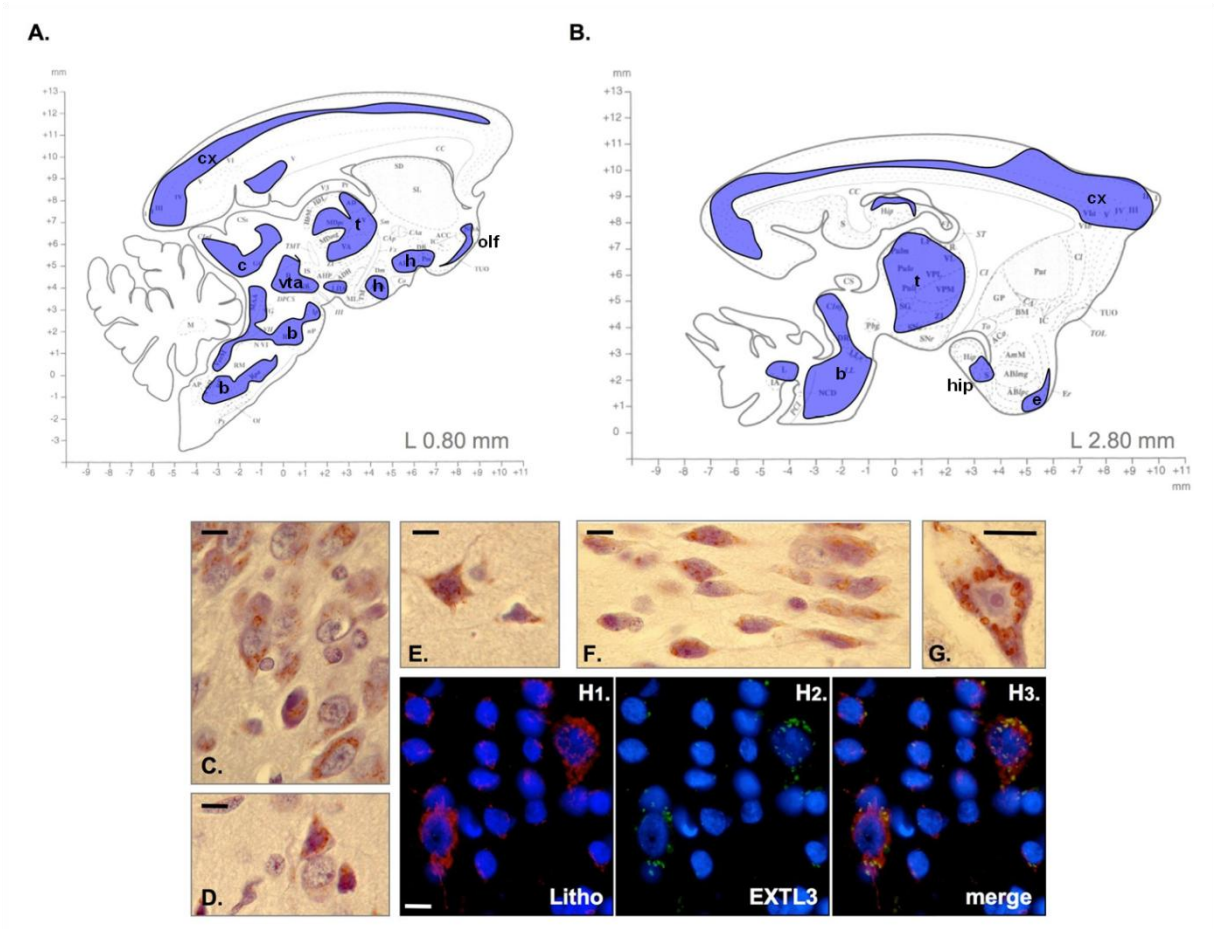
A.
B.
cx
olf
t
c
vta
h
b
L 0.80 mm
hip
e
L 2.80 mm
C.
D.
E.
F.
G.
H1.
H2.
H3.
Litho
EXTL3
merge

Fig.4

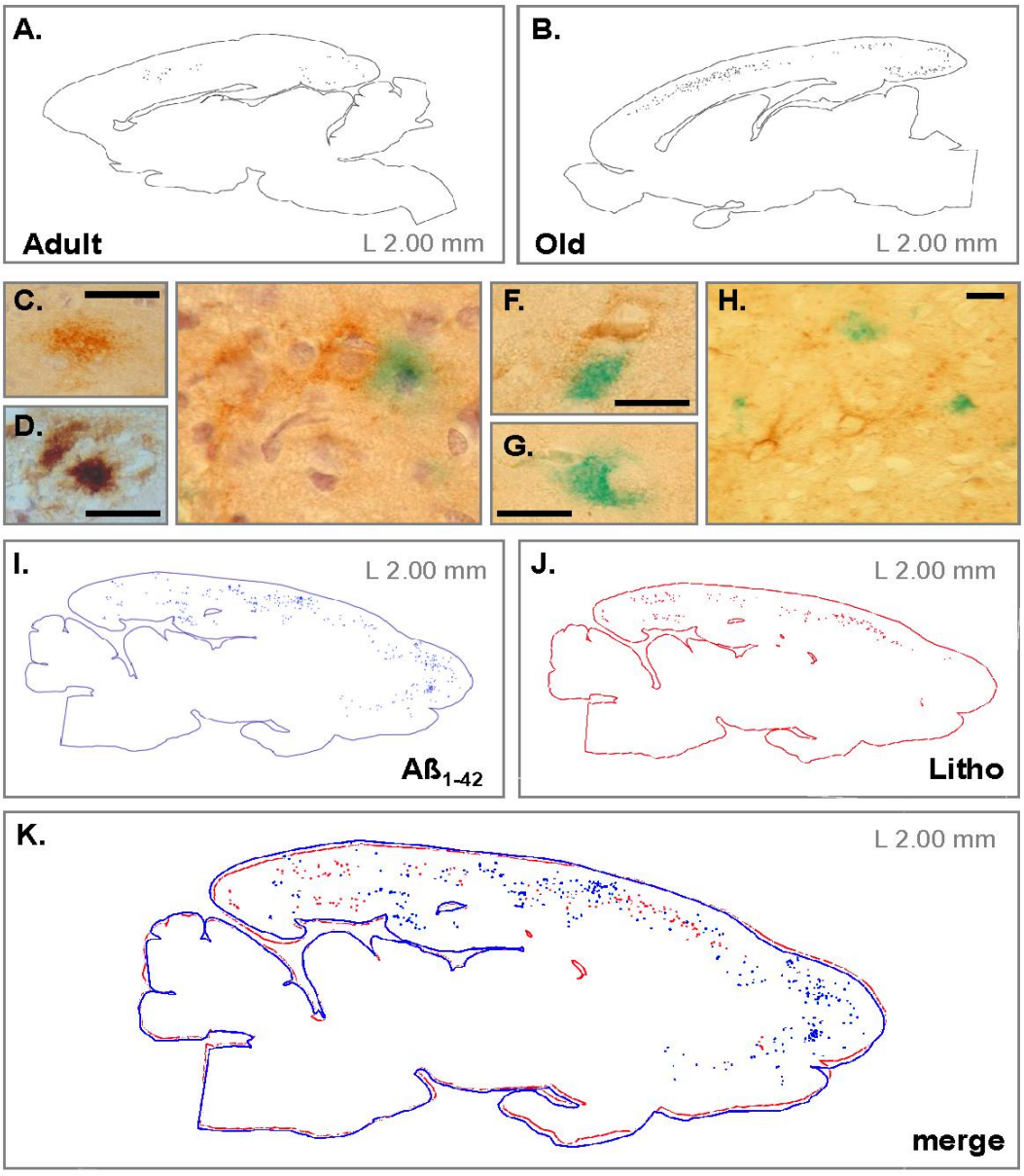
A.
Adult
L 2.00 mm
B.
Old
L 2.00 mm
C.
D.
F.
G.
H.
I.
L 2.00 mm
Aß1-42
J.
L 2.00 mm
Litho
K.
L 2.00 mm
merge

Fig.5

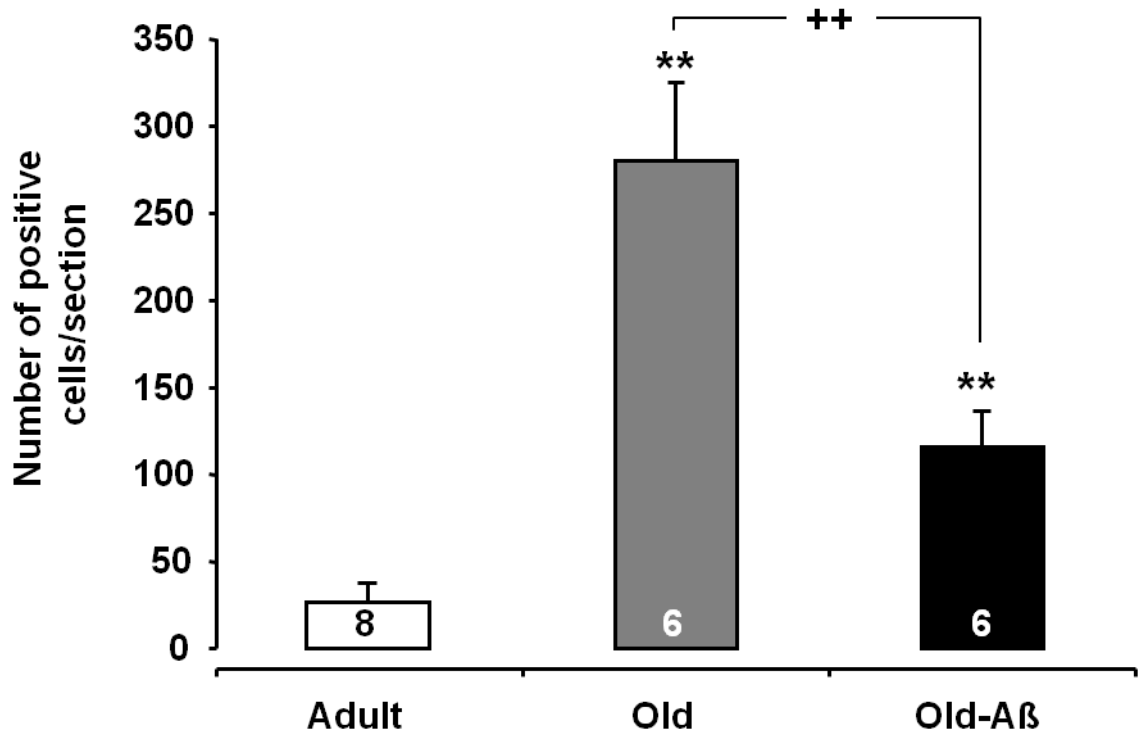
Number of positive cells/section
350
300
250
200
150
100
50
0
**
**
++
8
6
6
Adult
Old
Old-Aß